

Shear locking-free analysis of thick plates using Mindlin's theory

Y. I. Özdemir[†], S. Bekiroğlu[‡] and Y. Ayvaz^{‡†}

Department of Civil Engineering, Karadeniz Technical University, 61080 Trabzon, Turkey

(Received April 18, 2006, Accepted March 1, 2007)

Abstract. The purpose of this paper is to study shear locking-free analysis of thick plates using Mindlin's theory and to determine the effects of the thickness/span ratio, the aspect ratio and the boundary conditions on the linear responses of thick plates subjected to uniformly distributed loads. Finite element formulation of the equations of the thick plate theory is derived by using higher order displacement shape functions. A computer program using finite element method is coded in C++ to analyze the plates clamped or simply supported along all four edges. In the analysis, 8- and 17-noded quadrilateral finite elements are used. Graphs and tables are presented that should help engineers in the design of thick plates. It is concluded that 17-noded finite element converges to exact results much faster than 8-noded finite element, and that it is better to use 17-noded finite element for shear-locking free analysis of plates. It is also concluded, in general, that the maximum displacement and bending moment increase with increasing aspect ratio, and that the results obtained in this study are better than the results given in the literature.

Keywords: Thick plate; Mindlin's theory; finite element method; 8-noded finite element; 17-noded finite element; thickness/span ratio; aspect ratio; boundary conditions.

1. Introduction

Plates are structural elements which are commonly used in the building industry. A plate is called isotropic when its properties are the same in all directions, anisotropic when its properties are different in different directions and orthotropic when its properties differ in two mutually perpendicular directions.

A plate is considered to be a thin plate if the ratio of the plate thickness to the smaller span length is less than 1/20; it is considered to be a thick plate if this ratio is larger than 1/20 (Timosenko and Woinowsky-Krieger 1959, Ugural 1981).

The behavior of thick plates has been investigated by several researchers. Reissner (1947, 1950) derived expressions for moments and shear forces for isotropic elastic plates including the effects of shear deformation, rotatory inertia, and vertical stress σ_z by using a variational principle. Later Mindlin (1951) derived equations of motion for isotropic elastic plates including the effects of shear

[†] Research Assistant, E-mail: yaprakozdemir@hotmail.com

[‡] Research Assistant, E-mail: bekiroglu_serkan@yahoo.com

^{‡†} Professor, Corresponding author, E-mail: ayvaz@ktu.edu.tr

deformation and rotatory inertia and obtained the equations to calculate stresses of a plate. Ayvaz (1992) derived the equations of motions for orthotropic elastic plates using Hamilton's principle, but did not present any results.

Mindlin theory of the plates requires only C^0 continuity for the finite elements in the analysis of thin and thick plates. Therefore it appears as an alternative to the thin plate theory which also requires C^1 continuity. This requirement in the thin plate theory is solved easily if Mindlin theory is used in the analysis of thin plates. Despite the simple formulation of this theory, discretization of the plate by means of the finite element comes out to be an important parameter. In many cases, numerical solution can have lack of convergence, which is known as "shear-locking". Shear locking can be avoided by increasing the mesh size, i.e., using finer mesh, but if the thickness/span ratio is "too small" (Lövdina 1996), convergence may not be achieved even if the finer mesh is used for the first and second order displacement shape functions (4- and 8-noded elements)

In order to avoid this problem, the method of reduced and selective reduced integration (Wanji and Cheung 2000, Ozkul and Ture 2004) are chosen instead of the full integration. The same problem can also be prevented by using higher order displacement shape function, but no references have been found in the literature, which analyze shear-locking effect in terms of thickness/span ratios, mesh size and boundary condition by comparing with the results of the low order displacement shape function.

The purpose of this paper is to study shear locking-free analysis of thick plates using Mindlin's theory by using higher order displacement shape function and to determine the effects of various parameters such as the thickness/span ratio, mesh size, the aspect ratio and the boundary conditions on the linear responses of thick plates subjected to uniformly distributed loads. Finite element formulation of the equations of the thick plate theory is derived by using higher order displacement shape functions. A computer program using finite element method is coded in C++ 6.0 to analyze the plates considered. For the integration of finite element matrix Gauss numerical integration method for three and seven sampling points, that is the full integration, is used. 8- and 17-noded finite elements are used in the program. 17-noded finite element is obtained by using the fourth order polynomial for the shape function.

2. Mathematical model

In this study, the potential energy function is used to derive the equilibrium and constitutive equations. This function is given as follows

$$V = F - \iint p w_0 dx dy \quad (1)$$

Where F is the strain energy, p is the external load and w_0 is the displacement of the plate. F , the strain energy of the plate, is given as follows (Reissner 1947)

$$F = \iint_V (\sigma_x \varepsilon_x + \sigma_y \varepsilon_y + \sigma_z \varepsilon_z + \tau_{xy} \gamma_{xy} + \tau_{xz} \gamma_{xz} + \tau_{yz} \gamma_{yz}) dV - \bar{W} \quad (2)$$

where σ_x , σ_y , and σ_z are normal stresses; τ_{xy} , is shear stress; τ_{yz} , and τ_{xz} are transverse shear stresses; ε_x , ε_y , and ε_z are normal strains; γ_{xy} , is shear strains; γ_{yz} , and γ_{xz} are transverse shear strains; \bar{W} is

the complementary energy of the plate. The complementary energy of the plate, \bar{W} , is written as follows

$$\bar{W} = \frac{1}{2} \int_V (\sigma_x \varepsilon_x + \sigma_y \varepsilon_y + \sigma_z \varepsilon_z + \tau_{xy} \gamma_{xy} + \tau_{xz} \gamma_{xz} + \tau_{yz} \gamma_{yz}) dV \quad (3)$$

2.1 Equations for stress resultants

If internal stresses are written in a matrix form, the following equation for the stresses can be obtained.

$$\{\sigma\} = [E]\{\varepsilon\} \quad (4)$$

where $[E]$ is the elasticity matrix, $\{\varepsilon\}$ is the strain vector of the plate.

Matrix $[E]$ may be partitioned into

$$E = \begin{bmatrix} E_k & 0 \\ 0 & E_\gamma \end{bmatrix} \quad (5)$$

in which $[E_k]$ is of size 3×3 and $[E_\gamma]$ is of size 2×2 . $[E_k]$, and $[E_\gamma]$ can be written as follows (Weaver and Johnston 1984)

$$[E_k] = \begin{bmatrix} \frac{E}{(1-\nu^2)} & \frac{\nu E}{(1-\nu^2)} & 0 \\ \frac{\nu E}{(1-\nu^2)} & \frac{E}{(1-\nu^2)} & 0 \\ 0 & 0 & \frac{E}{2(1-\nu)} \end{bmatrix}; \quad [E_\gamma] = \begin{bmatrix} \frac{E}{2.4(1+\nu)} & 0 \\ 0 & \frac{E}{2.4(1+\nu)} \end{bmatrix} \quad (6)$$

If Eq. (6) is substituted into Eq. (5) and then into Eq. (4), Eq. (4) can be rewritten as follows

$$\begin{bmatrix} \sigma_x \\ \sigma_y \\ \tau_{xy} \\ \tau_{xz} \\ \tau_{yz} \end{bmatrix} = \begin{bmatrix} \frac{E}{(1-\nu^2)} & \frac{\nu E}{(1-\nu^2)} & 0 & 0 & 0 \\ \frac{\nu E}{(1-\nu^2)} & \frac{E}{(1-\nu^2)} & 0 & 0 & 0 \\ 0 & 0 & \frac{E}{2(1+\nu)} & 0 & 0 \\ 0 & 0 & 0 & \frac{E}{2.4(1+\nu)} & 0 \\ 0 & 0 & 0 & 0 & \frac{E}{2.4(1+\nu)} \end{bmatrix} \begin{bmatrix} \varepsilon_x \\ \varepsilon_y \\ \gamma_{xy} \\ \gamma_{xz} \\ \gamma_{yz} \end{bmatrix} \quad (7)$$

Generalized stresses are written in a matrix form and calculated as

$$\{M\} = [\bar{E}]\{\varepsilon\} \quad (8)$$

In terms of the internal stresses and strains, Eq. (8) can be written as follows (Cai *et al.* 2002)

$$\begin{Bmatrix} M_x \\ M_y \\ M_{xy} \\ Q_x \\ Q_y \end{Bmatrix} = \begin{Bmatrix} \int_{-t/2}^{t/2} \sigma_x z \\ \int_{-t/2}^{t/2} \sigma_y z \\ \int_{-t/2}^{t/2} \tau_{xy} z \\ \int_{-t/2}^{t/2} \tau_{xz} \\ \int_{-t/2}^{t/2} \tau_{yz} \end{Bmatrix} = [\bar{E}] \begin{Bmatrix} -\frac{\partial \varphi_x}{\partial x} \\ \frac{\partial \varphi_y}{\partial y} \\ \left(\frac{\partial \varphi_x}{\partial y} + \frac{\partial \varphi_y}{\partial x} \right) \\ -\varphi_x + \frac{\partial w}{\partial x} \\ \varphi_y + \frac{\partial w}{\partial y} \end{Bmatrix} = [\bar{E}] \begin{Bmatrix} \varepsilon_x \\ \varepsilon_y \\ \gamma_{xy} \\ \gamma_{xz} \\ \gamma_{yz} \end{Bmatrix} \quad (9)$$

Where $[\bar{E}]$, is the elasticity matrix and it is given as

$$[\bar{E}] = \begin{bmatrix} \bar{E}_k & 0 \\ 0 & \bar{E}_\gamma \end{bmatrix} \quad (10)$$

where

$$\begin{aligned} \bar{E}_k &= E_k \frac{t^3}{12} \\ \bar{E}_\gamma &= k E_\gamma t \end{aligned} \quad (11)$$

In this equation, t is the thickness of the plate, k is a constant to account for the actual nonuniformity of the shearing stresses.

2.2 Boundary conditions

In this study, since the plates considered are clamped or simply supported along all four edges, the following boundary conditions are used.

For clamped plates (Fig. 1);

Along $x = -a/2$ and $x = a/2$; $\varphi_x = 0$ and $w_0 = 0$.

Along $y = -b/2$ and $y = b/2$; $\varphi_y = 0$ and $w_0 = 0$.

For simply supported plates (see Fig. 1);

Along $x = -a/2$ and $x = a/2$; $M_x = 0$ and $w_0 = 0$.

Along $y = -b/2$ and $y = b/2$; $M_y = 0$ and $w_0 = 0$.

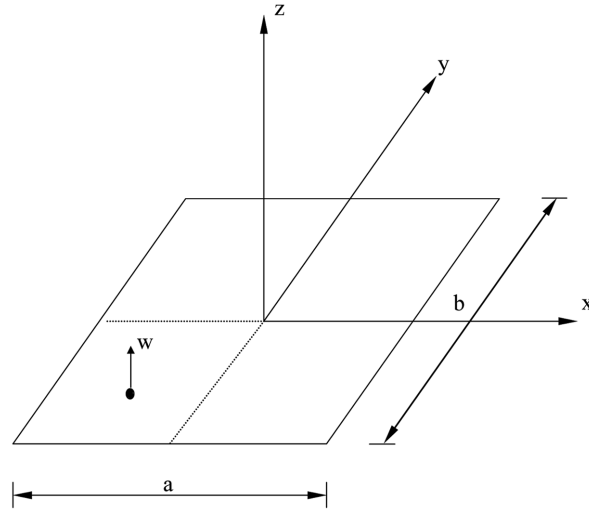


Fig. 1 The plate used in this study

3. Finite element formulation of the problem

The simplest type of plate-bending element has rectangular geometry which is a special case of quadrilateral geometry. In this study, two kinds of serendipity elements are used. One is 8-noded quadrilateral element (MT8) and the other one is 17-noded quadrilateral element (MT17) (Fig. 2).

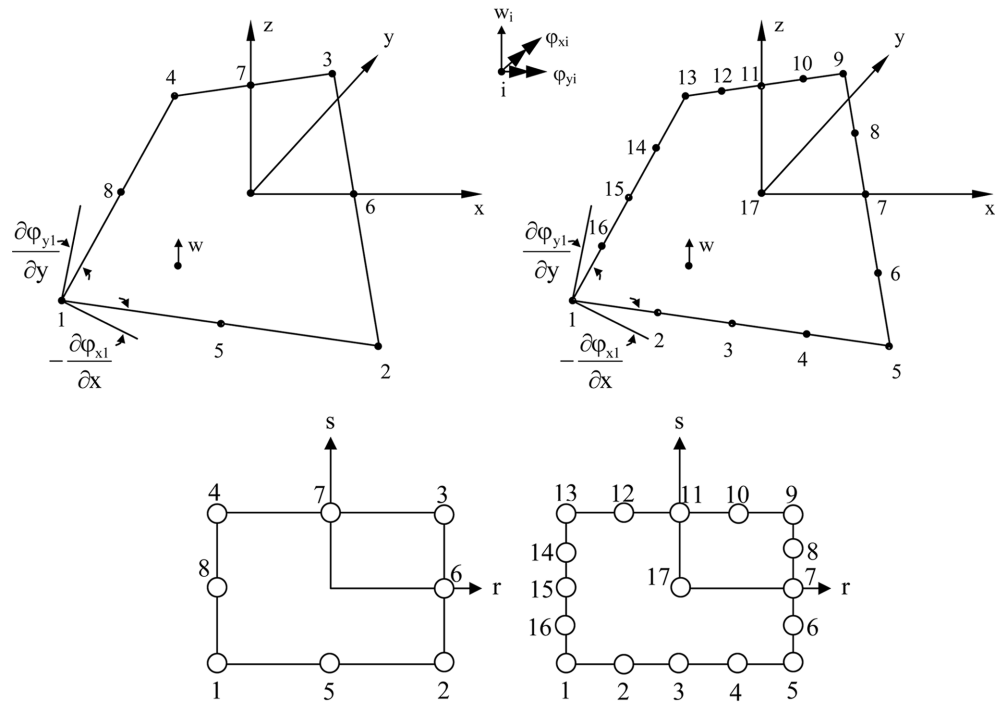


Fig. 2 8- (second order), and 17-noded (fourth order) quadrilateral finite elements used in this study

The nodal displacements for these elements can be written as follows

$$u = \{u, v, w\} = \{-z\varphi_x, z\varphi_y, w\} = \left\{ -z\frac{\partial\varphi_i}{\partial x}, z\frac{\partial\varphi_i}{\partial y}, w \right\} \quad (12)$$

$$u = -z\varphi_x = -z \sum_1^{8 \text{ or } 17} h_i \varphi_{xi}, \quad v = z\varphi_y = z \sum_1^{8 \text{ or } 17} h_i \varphi_{yi}, \quad w = \sum_1^{8 \text{ or } 17} h_i w_i \quad \begin{array}{l} i = 1, \dots, 8 \text{ for 8-noded element} \\ i = 1, \dots, 17 \text{ for 17-noded element} \end{array} \quad (13)$$

where w is the displacement, and φ_x and φ_y are the rotations in the x and y directions, respectively. Nodal actions corresponding to the displacements in Eq. (12) are

$$p_i = \{p_{i1}, p_{i2}, p_{i3}\} = \{M_{xi}, M_{yi}, p_{zi}\} \quad \begin{array}{l} i = 1, \dots, 8 \text{ for 8-noded element} \\ i = 1, \dots, 17 \text{ for 17-noded element} \end{array} \quad (14)$$

The symbols p_{zi} denotes a force in the z direction, but M_{xi} and M_{yi} are the moments in the x and y directions, respectively. Note that these fictitious moments at the nodes are not the same as the distributed moments in the vector M of generalized stresses (Weaver and Johnston 1984).

The displacement function chosen for those elements are

$$\begin{aligned} w &= c_1 + c_2r + c_3s + c_4r^2 + c_5rs + c_6s^2 + c_7r^2s + c_8rs^2 \\ w &= c_1 + c_2r + c_3s + c_4r^2 + c_5rs + c_6s^2 + c_7r^2s + c_8rs^2 + c_9r^3 + c_{10}r^3s + c_{11}rs^3 \\ &\quad + c_{12}s^3 + c_{13}r^2s^2 + c_{14}r^4 + c_{15}r^4s + c_{16}rs^4 + c_{17}s^4 \end{aligned} \quad (15)$$

From this assumption, it is possible to derive the displacement shape function to be

$$\begin{aligned} h &= [h_1, h_2, h_3, h_4, h_5, h_6, h_7, h_8] \quad \text{for 8-noded element} \\ h &= [h_1, \dots, h_{17}] \quad \text{for 17-noded element} \end{aligned} \quad (16)$$

where

$$\begin{aligned} h_1 &= \left(\frac{1}{4}\right)*(1-r)*(1-s)*(-r-s-1), \quad h_2 = \left(\frac{1}{2}\right)*(1-r*s)*(1-s) \\ h_3 &= \left(\frac{1}{4}\right)*(1+r)*(1-s)*(r-s-1), \quad h_4 = \left(\frac{1}{2}\right)*(1+r)*(1-s*s) \\ h_5 &= \left(\frac{1}{4}\right)*(1+r)*(1+s)*(r+s-1), \quad h_6 = \left(\frac{1}{2}\right)*(1-r*s)*(1+s) \\ h_7 &= \left(\frac{1}{4}\right)*(1-r)*(1+s)*(-r+s-1), \quad h_8 = \left(\frac{1}{2}\right)*(1-r)*(1-s*s) \end{aligned} \quad (17)$$

for 8-noded finite element. The similar displacement shape functions for 17-noded element can be obtained, and they are given as follows

$$\begin{aligned} h_1 &= \left(\frac{1}{3}\right)r + \left(\frac{1}{3}\right)s - \left(\frac{5}{12}\right)r*s - \left(\frac{1}{3}\right)r^2 + \left(\frac{1}{12}\right)r^2*s + \left(\frac{1}{12}\right)r*s^2 - \left(\frac{1}{3}\right)s^2 - \left(\frac{1}{3}\right)r^3 + \left(\frac{1}{3}\right)r^3*s \\ &\quad + \left(\frac{1}{3}\right)r*s^3 - \left(\frac{1}{3}\right)s^3 + \left(\frac{1}{4}\right)r^2*s^2 + \left(\frac{1}{3}\right)r^4 - \left(\frac{1}{3}\right)r^4*s - \left(\frac{1}{3}\right)r*s^4 + \left(\frac{1}{3}\right)r^4 \end{aligned}$$

$$\begin{aligned}
h_2 &= -\left(\frac{2}{3}\right)r + \left(\frac{2}{3}\right)r^*s + \left(\frac{4}{3}\right)r^2 - \left(\frac{4}{3}\right)r^2*s + \left(\frac{2}{3}\right)r^3 - \left(\frac{2}{3}\right)r^3*s - \left(\frac{4}{3}\right)r^4 + \left(\frac{4}{3}\right)r^4*s \\
h_3 &= -\left(\frac{1}{2}\right)s - (2)r^2 + \left(\frac{5}{2}\right)r^2*s + \left(\frac{1}{2}\right)s^2 - \left(\frac{1}{2}\right)r^2*s^2 + (2)r^4 - (2)r^4*s \\
h_4 &= \left(\frac{2}{3}\right)r - \left(\frac{2}{3}\right)r*s + \left(\frac{4}{3}\right)r^2 - \left(\frac{4}{3}\right)r^2*s - \left(\frac{2}{3}\right)r^3 + \left(\frac{2}{3}\right)r^3*s - \left(\frac{4}{3}\right)r^4 + \left(\frac{4}{3}\right)r^4*s \\
h_5 &= -\left(\frac{1}{3}\right)r + \left(\frac{1}{3}\right)s + \left(\frac{5}{12}\right)r*s - \left(\frac{1}{3}\right)r^2 + \left(\frac{1}{12}\right)r^2*s - \left(\frac{1}{12}\right)r^2*s^2 - \left(\frac{1}{3}\right)s^2 + \left(\frac{1}{3}\right)r^3 - \left(\frac{1}{3}\right)r^3*s \\
&\quad - \left(\frac{1}{3}\right)r*s^3 - \left(\frac{1}{3}\right)s^3 + \left(\frac{1}{4}\right)r^2*s^2 + \left(\frac{1}{3}\right)r^4 - \left(\frac{1}{3}\right)r^4*s + \left(\frac{1}{3}\right)r*s^4 + \left(\frac{1}{3}\right)s^4 \\
h_6 &= -\left(\frac{2}{3}\right)s + \left(\frac{2}{3}\right)r*s + \left(\frac{4}{3}\right)r*s^2 + \left(\frac{4}{3}\right)s^2 + \left(\frac{2}{3}\right)r*s^3 + \left(\frac{2}{3}\right)s^3 - \left(\frac{4}{3}\right)r*s^4 - \left(\frac{4}{3}\right)s^4 \\
h_7 &= \left(\frac{1}{2}\right)r + \left(\frac{1}{2}\right)r^2 - \left(\frac{5}{2}\right)r*s^2 - (2)s^2 - \left(\frac{1}{2}\right)r^2*s^2 + (2)r*s^4 + (2)s^4 \\
h_8 &= \left(\frac{2}{3}\right)s + \left(\frac{2}{3}\right)r*s + \left(\frac{4}{3}\right)r*s^2 + \left(\frac{4}{3}\right)s^2 - \left(\frac{2}{3}\right)r*s^3 - \left(\frac{2}{3}\right)s^3 - \left(\frac{4}{3}\right)r*s^4 - \left(\frac{4}{3}\right)r^4 \\
h_9 &= -\left(\frac{1}{3}\right)r - \left(\frac{1}{3}\right)s - \left(\frac{5}{12}\right)r*s - \left(\frac{1}{3}\right)r^2 - \left(\frac{1}{12}\right)r^2*s - \left(\frac{1}{12}\right)r^2*s^2 - \left(\frac{1}{3}\right)s^2 + \left(\frac{1}{3}\right)r^3 + \left(\frac{1}{3}\right)r^3*s \\
&\quad + \left(\frac{1}{3}\right)r*s^3 + \left(\frac{1}{3}\right)s^3 + \left(\frac{1}{4}\right)r^2*s^2 + \left(\frac{1}{3}\right)r^4 + \left(\frac{1}{3}\right)r^4*s + \left(\frac{1}{3}\right)r*s^4 + \left(\frac{1}{3}\right)s^4 \\
h_{10} &= \left(\frac{2}{3}\right)r + \left(\frac{2}{3}\right)r*s + \left(\frac{4}{3}\right)r^2 + \left(\frac{4}{3}\right)r^2*s - \left(\frac{2}{3}\right)r^3 - \left(\frac{2}{3}\right)r^3*s - \left(\frac{4}{3}\right)r^4 - \left(\frac{4}{3}\right)r^4*s \\
h_{11} &= \left(\frac{1}{2}\right)s - (2)r^2 - \left(\frac{5}{2}\right)r^2*s + \left(\frac{1}{2}\right)s^2 - \left(\frac{1}{2}\right)r^2*s^2 + (2)r^4 + (2)r^4*s \\
h_{12} &= -\left(\frac{2}{3}\right)r - \left(\frac{2}{3}\right)r*s + \left(\frac{4}{3}\right)r^2 + \left(\frac{4}{3}\right)r^2*s + \left(\frac{2}{3}\right)r^3 + \left(\frac{2}{3}\right)r^3*s - \left(\frac{4}{3}\right)r^4 - \left(\frac{4}{3}\right)r^4*s \\
h_{13} &= \left(\frac{1}{3}\right)r - \left(\frac{1}{3}\right)s + \left(\frac{5}{12}\right)r*s - \left(\frac{1}{3}\right)r^2 - \left(\frac{1}{12}\right)r^2*s + \left(\frac{1}{12}\right)r^2*s^2 - \left(\frac{1}{3}\right)s^2 - \left(\frac{1}{3}\right)r^3 - \left(\frac{1}{3}\right)r^3*s \\
&\quad - \left(\frac{1}{3}\right)r*s^3 + \left(\frac{1}{3}\right)s^3 + \left(\frac{1}{4}\right)r^2*s^2 + \left(\frac{1}{3}\right)r^4 + \left(\frac{1}{3}\right)r^4*s - \left(\frac{1}{3}\right)r*s^4 + \left(\frac{1}{3}\right)s^4 \\
h_{14} &= \left(\frac{2}{3}\right)s - \left(\frac{2}{3}\right)r*s - \left(\frac{4}{3}\right)r*s^2 + \left(\frac{4}{3}\right)s^2 + \left(\frac{2}{3}\right)r*s^3 - \left(\frac{2}{3}\right)s^3 + \left(\frac{4}{3}\right)r*s^4 - \left(\frac{4}{3}\right)s^4 \\
h_{15} &= -\left(\frac{1}{2}\right)r + \left(\frac{1}{2}\right)r^2 + \left(\frac{5}{2}\right)r^2*s^2 - (2)s^2 - \left(\frac{1}{2}\right)r^2*s^2 - (2)r*s^4 + (2)s^4 \\
h_{16} &= -\left(\frac{2}{3}\right)s + \left(\frac{2}{3}\right)r*s - \left(\frac{4}{3}\right)r*s^2 + \left(\frac{4}{3}\right)s^2 - \left(\frac{2}{3}\right)r*s^3 + \left(\frac{2}{3}\right)s^3 + \left(\frac{4}{3}\right)r*s^4 - \left(\frac{4}{3}\right)s^4
\end{aligned}$$

$$h_{17} = 1 - r^2 - s^2 + r^2 * s^2 \quad (18)$$

The subscripts in the vector of h stand for the node number of 8- or 17-noded quadrilateral finite element.

For transforming local coordinates to the global coordinates, the Jacobian matrix is required. The 3×3 Jacobian matrix required in this formulation is

$$[J] = \begin{bmatrix} x_r & y_r & 0 \\ x_s & y_s & 0 \\ 0 & 0 & 1 \end{bmatrix} \quad (19)$$

where r and s are the local coordinates of the plate, x_r, x_s, y_r, y_s are the derivatives with respect to local coordinates. x_i, y_i are global coordinates of the nodes of the plate. The derivatives with respect to local coordinates are given as

$$\begin{aligned} x_r &= \sum_{i=1}^{8 \text{ or } 17} (h_{i,r} x_i) \dots y_r = \sum_{i=1}^{8 \text{ or } 17} (h_{i,r} y_i) \\ x_s &= \sum_{i=1}^{8 \text{ or } 17} (h_{i,s} x_i) \dots y_s = \sum_{i=1}^{8 \text{ or } 17} (h_{i,s} y_i) \end{aligned} \quad (20)$$

After Eq. (20) is substituted into Eq. (18), the inverse of J can be obtained to be

$$[J]^{-1} = \begin{bmatrix} r_x & s_x & 0 \\ r_y & s_y & 0 \\ 0 & 0 & 1 \end{bmatrix} \quad (21)$$

Certain derivatives are required with respect to local coordinates, which are collected into a 3×3 matrix

$$\begin{bmatrix} u_r & v_r & w_r \\ u_s & v_s & w_s \\ u_z & v_z & w_z \end{bmatrix} = \sum_{i=1}^{8 \text{ or } 17} \begin{bmatrix} -z h_{i,r} \varphi_{xi} & z h_{i,r} \varphi_{yi} & h_{i,r} w_i \\ -z h_{i,s} \varphi_{xi} & z h_{i,s} \varphi_{yi} & h_{i,s} w_i \\ -h_i \varphi_{xi} & h_i \varphi_{yi} & 0 \end{bmatrix} \quad (22)$$

Transformation of these derivatives to global coordinates is accomplished using the inverse of the Jacobian matrix, and it is given as follows

$$\begin{bmatrix} u_x & v_x & w_x \\ u_y & v_y & w_y \\ u_z & v_z & w_z \end{bmatrix} = J^{-1} \begin{bmatrix} u_r & v_r & w_r \\ u_s & v_s & w_s \\ u_z & v_z & w_z \end{bmatrix} \quad (23)$$

The strain vector in Eq. (7) for these elements can be rewritten as follows

$$\{\varepsilon\} = \begin{bmatrix} \varepsilon_x \\ \varepsilon_y \\ \gamma_{xy} \\ \gamma_{xz} \\ \gamma_{yz} \end{bmatrix} = \begin{bmatrix} u_x \\ v_y \\ u_y + v_x \\ u_z + w_x \\ v_z + w_y \end{bmatrix} \quad (24)$$

For the stresses corresponding to the strains, see Eq. (7).

Before formulating element stiffness matrix, strain-displacement matrix B is partitioned as follows

$$[B] = \begin{bmatrix} B_k \\ B_\gamma \end{bmatrix} = \begin{bmatrix} z \bar{B}_k \\ B_\gamma \end{bmatrix} \quad (25)$$

Where B_k has the size of 3×24 , 3×51 for 8- and 17-noded quadrilateral elements, respectively and B_γ has the size of 2×24 , 2×51 for 8- and 17-noded quadrilateral elements, respectively. The matrix B for each element can be written as follow

$$[B] = \begin{bmatrix} 0 & 0 & -\frac{\partial h_i}{\partial x} & \dots \\ 0 & \frac{\partial h_i}{\partial y} & 0 & \dots \\ 0 & \frac{\partial h_i}{\partial x} & -\frac{\partial h_i}{\partial y} & \dots \\ \frac{\partial h_i}{\partial x} & 0 & -h_i & \dots \\ \frac{\partial h_i}{\partial y} & h_i & 0 & \dots \end{bmatrix}_{\substack{5 \times 24 \text{ for 8-noded element} \\ 5 \times 51 \text{ for 17-noded element}}} \quad i = 1, \dots, 8 \text{ for 8-noded element} \\ i = 1, \dots, 17 \text{ for 17-noded element} \quad (26)$$

The details of the matrices B for 8- and 17-noded quadrilateral finite elements are presented in APPENDIX. Then the stiffness matrices for these elements are written as (Cook *et al.* 1989)

$$K = \int_V E B dV = \int_V [z \bar{B}_k^T \ B_\gamma^T] \begin{bmatrix} E_k & 0 \\ 0 & E_\gamma \end{bmatrix} \begin{bmatrix} z \bar{B}_k \\ B_\gamma \end{bmatrix} dV$$

$$K = \int_V (z^2 \bar{B}_k^T E_k \bar{B}_k + (\bar{B}_\gamma^T E_\gamma \bar{B}_\gamma)) dV \quad (27)$$

Integration of Eq. (27) through the thickness yields

$$K = \int_A (\bar{B}_k^T E_k \bar{B}_k + \bar{B}_\gamma^T E_\gamma \bar{B}_\gamma) dA \quad (28)$$

Thus,

$$K = \int_A \bar{B}^T \bar{E} \bar{B} dA = \int_{-1}^1 \int_{-1}^1 \bar{B}^T \bar{E} \bar{B} |J| dr ds \quad (29)$$

which must be evaluated numerically (Bathe 1996).

The matrices which show the displacements and rotations in the plate are given as follows

$$\begin{aligned} \hat{u}^T &= [\varphi_{x1} \ \varphi_{y1} \ w_1; \dots; \varphi_{x8} \ \varphi_{y8} \ w_8] \\ \hat{u}^T &= [\varphi_{x1} \ \varphi_{y1} \ w_1; \dots; \varphi_{x17} \ \varphi_{y17} \ w_{17}] \end{aligned} \quad (30)$$

The values of these matrices can be calculated with the Gauss Integration method. 3 gauss points for 8-noded finite element and 7 gauss points for 17-noded finite element are sufficient. Then the strains are calculated by the following equation.

$$\{\varepsilon\} = [B]\{u\} \quad (31)$$

After finding the strains, the stresses of the plate can be calculated by Eq. (4).

4. Numerical examples

4.1 Data

A number of examples are taken to examine the performance of the element of MT8, and MT17 which include tests on convergence of both displacements and stresses with a derived computer program.

A square plate which is subjected to a uniformly distributed load is modeled with two different boundary conditions, i.e., either simply supported or clamped along all four edges, to evaluate the convergence of the solutions obtained with MT8 and MT17 elements. The geometric and material properties used are $E = 2.7 * 10^6$ kN/m², $\nu = 0.3$, $a = 3$ m, $q_z = 20$ kN/m², and $k = 5/6$, where q_z is the uniformly distributed load, and a is the smaller span length of the plate. In the analysis, the full plate is used.

Since the method used herein is a numerical method, the finite element method, there is always some error in the results, depending on the mesh size used to solve the problem. Therefore, for the sake of accuracy in the results, rather than starting with a finite element mesh size, the mesh size to produce the desired accuracy is determined. To find out the required mesh size, convergence of the maximum displacement is checked for different mesh sizes. Maximum displacements coefficients obtained from these different meshes are given in Fig. 3. In conclusion, as seen from Fig. 3, the results have an acceptable error when using 4×4 divisions (16 elements) for MT17 element and 16×16 divisions (256 elements) for MT8 element for a square plate. But for the comparisons with other studies, various mesh sizes are used. As the aspect ratio changes, the lengths of the divisions are kept the same as in the square plate by increasing the element number in the long direction.

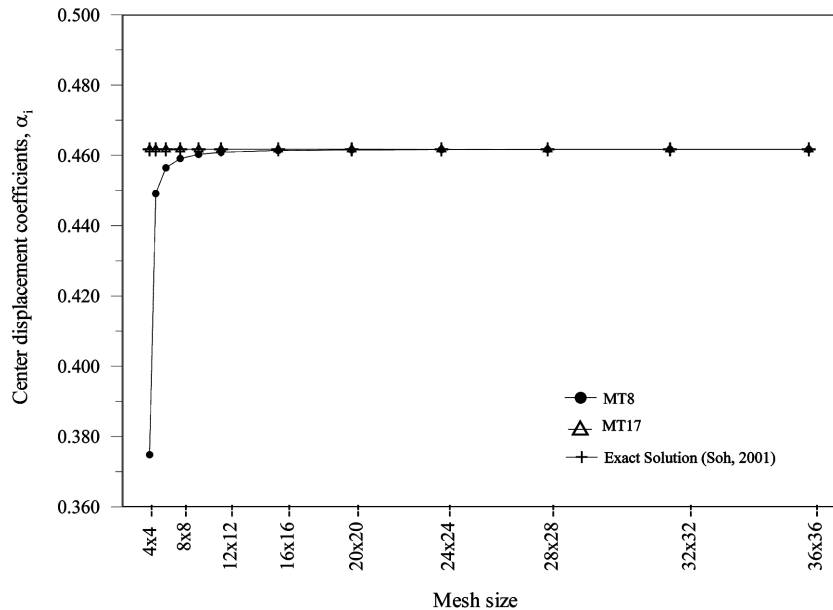


Fig. 3 Maximum displacement of the simply supported plates with different mesh sizes

4.2 Results

In this study, the maximum displacement and bending moment coefficients for different thickness/span ratios and the maximum displacements and bending moments for different aspect ratios are presented. This simplification to maximum responses is supported by the fact that maximum values of these quantities are the most important ones for design.

In order to understand better the linear response of thick plates subjected to uniformly distributed loads, the results are presented in tables and graphs. The maximum displacement and bending moment coefficients for different thickness/span ratios and mesh sizes, and the maximum bending moment coefficient for different thickness/span ratios are given in Tables 1, 2, and 3, respectively, for clamped plates. The maximum displacement and bending moment coefficient for different mesh sizes are given in Table 4 for simply supported plates. These values are also presented in graphical form in Figs. 4, 5, and 6, respectively.

As seen from Tables 1, 2, and Fig. 4, center displacement coefficients, α_i , of the clamped plates obtained in this study are very close to the exact solution.

As seen from Table 3, center moment coefficients, β_i , of the clamped plates obtained in this study with both element types are very close to the exact solution of thin plate.

As seen from Table 4 and Fig. 5, center displacement coefficients, α_i , of the simply supported plates obtained in this study are very close to the exact solution. As also seen from Table 4 and Fig. 5, the results obtained by using 17-noded finite element almost coincide with the exact result for any mesh sizes. The solutions obtained in this study for thick plate coincide with the exact solution if 8×8 mesh sizes (64 elements) are used for MT17 element and 32×32 mesh sizes (1024 elements) are used for MT8 element.

Table 1 Center displacements coefficients, α_i , ($=\omega/(qa^4/100D)$) of the clamped square plate for different mesh sizes and t/a ratios

t/a	α_i						Exact, Soh (2001)	
	This study (MT8,24 dof.)			This study (MT17,51 dof.)				
	Mesh size		Mesh size					
	4 × 4	8 × 8	16 × 16	4 × 4	8 × 8	16 × 16		
0.001	0.0005	0.0499	0.1227	0.1011	0.1252	0.1265	0.1265	
0.01	0.0359	0.1189	0.1256	0.1230	0.1268	0.1268	0.1265	
0.10	0.1420	0.1499	0.1504	0.1503	0.1505	0.1505	0.1499	
0.15	0.1745	0.1785	0.1787	0.1786	0.1788	0.1788	0.1798	
0.20	0.2146	0.2170	0.2172	0.2171	0.2172	0.2172	0.2167	
0.25	0.2639	0.2657	0.2658	0.2657	0.2658	0.2658	-	
0.30	0.3230	0.3245	0.3246	0.3245	0.3246	0.3246	0.3227	
0.35	0.3922	0.3936	0.3937	0.3935	0.3937	0.3937	0.3951	

Table 2 Center displacements coefficients, α_i , ($=\omega/(qa^4/100D)$) of the clamped square plate for different t/a ratios

t/a	α_i						Exact, Soh (2001)		
	Çelik (1996)	Yuqi and Fei (1992)	Yua and Miller (1988)	Yua and Miller (1989)	Owen and Zienkiewicz (1982)	Soh (2001)			
0.001	0.1265	0.1293	0.1234	0.1255	0.1220	0.1279	0.1118	0.1252	0.1265
0.01	0.1284	0.1293	0.1236	0.1267	0.1230	0.1281	0.1241	0.1268	0.1265
0.10	0.1584	0.1521	0.1482	0.1513	0.1460	0.1514	0.1505	0.1487	0.1499
0.15	0.1859	0.1801	0.1776	0.1807	-	-	0.1788	0.1779	0.1798
0.20	0.2236	0.2181	0.2171	0.2203	0.2110	0.2183	0.2172	0.2167	0.2167
0.25	0.2716	0.2658	-	0.2700	-	-	0.2658	0.2655	-
0.30	0.3299	0.3229	-	-	-	0.3259	0.3246	0.3243	0.3227
0.35	0.3987	0.3896	-	-	-	0.3952	0.3937	0.3934	0.3951

Table 3 Maximum bending moment coefficients, β_i , ($=M_x/(qa^2/10)$) at the center of the clamped square plates

t/a	β_i						Exact (Thin plate) (Owen and Zienkiewicz 1982)
	Çelik (1996) (16 dof.) (20 × 20 meshes)	Owen and Zienkiewicz (1982)	Soh (2001)	This study MT8 (24 dof.) (12 × 12 meshes)	This study MT8 (24 dof.) (20 × 20 meshes)	This study MT17 (51 dof.) (8 × 8 meshes)	
0.001	0.2300	0.2270	0.2069	0.2249	0.2111	0.2209	0.231
0.01	0.2340	0.2270	0.2069	0.2280	0.2267	0.2290	0.231
0.10	0.253	0.236	0.2070	0.2325	0.2324	0.2320	0.231
0.15	0.254	-	-	0.2359	0.2346	0.2340	0.231
0.20	0.255	0.250	0.2071	0.2382	0.2364	0.2357	0.231
0.25	0.255	-	-	0.2399	0.2377	0.2370	0.231
0.30	0.255	-	-	0.2411	0.2387	0.2380	0.231
0.35	0.255	-	-	0.2420	0.2394	0.2386	0.231

Table 4 Center displacements coefficients, α_i , ($=\omega/(qa^4/100D)$) and bending moment coefficients, β_i , ($=M/(qa^2/10)$) of the simply supported square plates for different mesh sizes and t/a ratios

a) Thickness/span ratio (t/a) = 0.001

Mesh	α_i					β_i				
	Soh (2001)	Batoz and Tahar (1982)	Zienkiewicz <i>et al.</i> (1993)	This study MT8	This study MT17	Soh (2001)	Batoz and Tahar (1982)	Zienkiewicz <i>et al.</i> (1993)	This study MT8	This study MT17
4 × 4	0.4045	0.4045	0.4593	0.0513	0.4004	0.5009	0.5005	0.5649	0.0616	0.4721
8 × 8	0.4060	0.4060	0.4292	0.3747	0.4062	0.4839	0.4839	0.5010	0.4454	0.4776
16 × 16	0.4062	0.4062	0.4164	0.4053	0.4063	0.4801	0.4801	0.4876	0.4775	0.4781
32 × 32	0.4062	0.4062	0.4110	0.4062	0.4063	0.4792	0.4792	0.4830	0.4785	0.4790
Exact, thick (Soh 2001)			0.4066					0.4792		
Exact, thin (Panc 1975)			0.4062					0.4789		

b) Thickness/span ratio (t/a) = 0.01

Mesh	α_i					β_i				
	Soh (2001)	Ibrahimbegovic (1993)	Zienkiewicz <i>et al.</i> (1993)	This study MT8	This study MT17	Soh (2001)	Ibrahimbegovic (1993)	Zienkiewicz <i>et al.</i> (1993)	This study MT8	This study MT17
4 × 4	0.4047	0.4461	0.4596	0.3735	0.4072	0.5007	0.5659	0.5649	0.4405	0.4763
8 × 8	0.4062	0.4227	0.4297	0.4051	0.4083	0.4842	0.5081	0.5012	0.4766	0.4805
16 × 16	0.4064	0.4140	0.4172	0.4075	0.4093	0.4804	0.4892	0.4882	0.4797	0.4811
32 × 32	0.4067	0.4106	0.4124	0.4087	0.4098	0.4797	0.4835	0.4841	0.4808	0.4820
Exact, thick (Soh 2001)			0.4099					0.4820		
Exact, thin (Panc 1975)			0.4064					0.4789		

c) Thickness/span ratio (t/a) = 0.1

Mesh	α_i					β_i							
	Soh (2001)	Ibrahimbegovic (1993)	Zienkiewicz <i>et al.</i> (1993)	Belouanar and Guenfoud (2005)	Cen <i>et al.</i> (2006)	This study MT8	This study MT17	Soh (2001)	Ibrahimbegovic (1993)	Zienkiewicz <i>et al.</i> (1993)	Cen <i>et al.</i> (2006)	This study MT8	This study MT17
4 × 4	0.4280	0.4774	0.4957	0.3587	0.4358	0.4491	0.4611	0.5206	0.5808	0.5694	0.5067	0.5011	0.5091
8 × 8	0.4419	0.4612	0.4727	0.4311	0.4437	0.4591	0.4617	0.5087	0.5238	0.5169	0.5034	0.5076	0.5095
16 × 16	0.4544	0.4600	0.4644	0.4525	0.4543	0.4614	0.4617	0.5081	0.5117	0.5117	0.5061	0.5094	0.5096
32 × 32	0.4596	0.4610	0.4624	-	0.4595	0.4617	0.4617	0.5091	0.5099	0.5100	0.5084	0.5096	0.5096
Exact, thick (Soh 2001)			0.4617							0.5096			
Exact, thin (Panc 1975)			0.4273							0.4789			

As seen from Table 4 and Fig. 6, center moment coefficients, β_i , of the simply supported plates obtained in this study are very close to the exact solution. As also seen from Table 4 and Fig. 6, the results obtained by using 17-noded finite element almost coincide with the exact result for any mesh

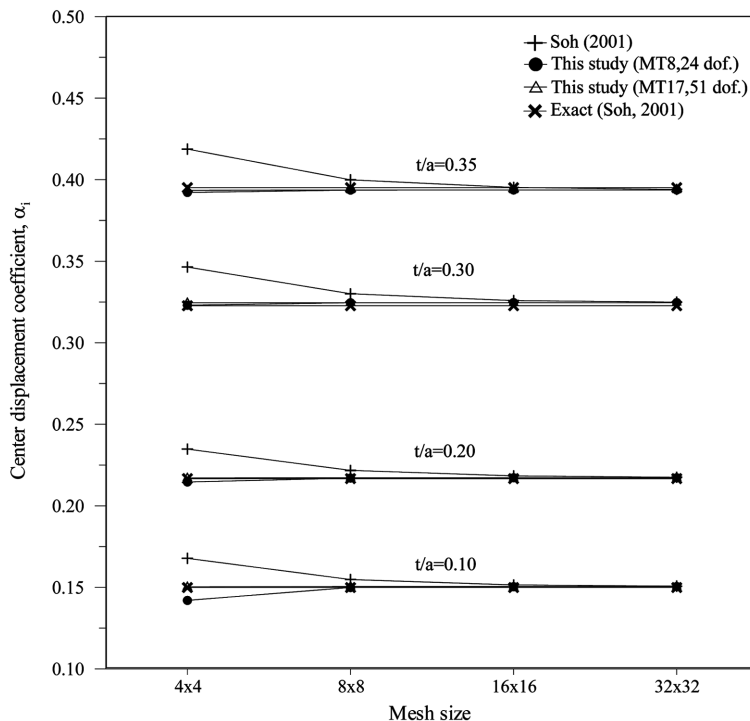


Fig. 4 Center displacement coefficients, α_i , of the clamped square plates for different thickness/span ratios, and mesh sizes

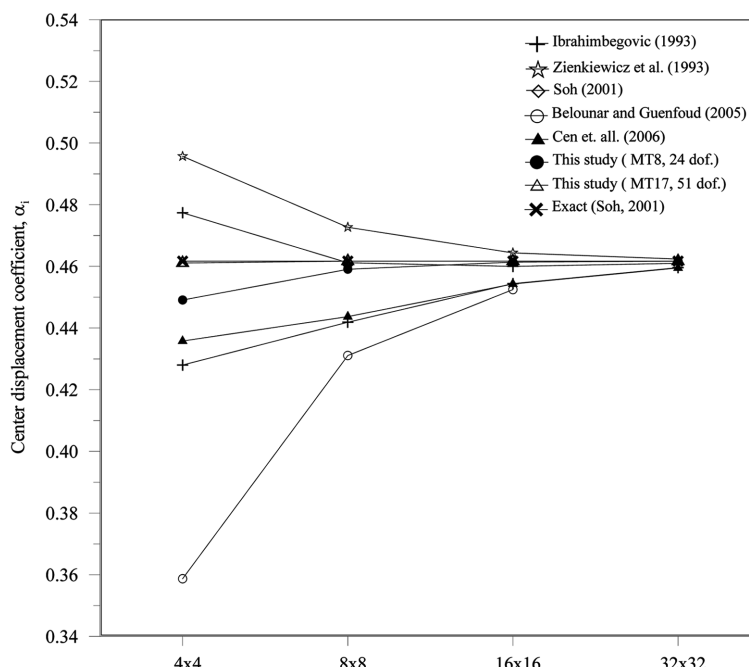


Fig. 5 Center displacement coefficients, α_i , of the simply supported square plates for different mesh sizes ($t/a = 0.1$)

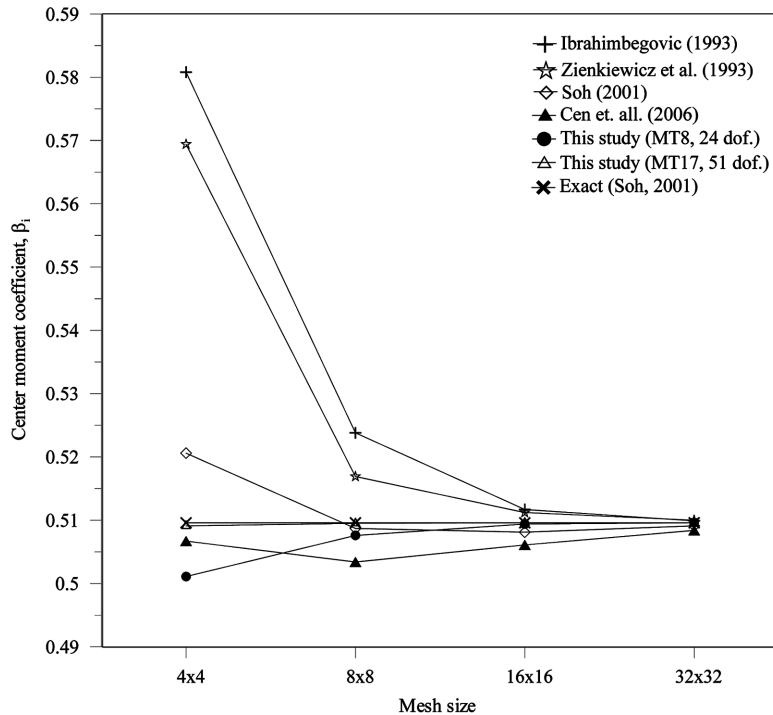


Fig. 6 Center moment coefficients, β_i , of the simply supported square plates for different mesh sizes ($t/a = 0.1$)

sizes. The solutions obtained for thick plate in this study coincide with the exact solution if 16×16 mesh sizes (256 elements) are used for MT17 element and 32×32 mesh sizes (1024 elements) are used for MT8 element.

As seen from Tables 1, 2, 3, and 4, and Figs. 4, 5, and 6, the results obtained in this study by using MT17 element converges rapidly to the exact results than the results given in the literature. By using this element, the mesh size required to produce the desired accuracy can be approximately reduced to the half of those of the given in the other literature, (Ibrahimbegovic 1993, Zienkiewicz 1993, Soh 2001).

As seen from the tables and figures given above, shear-locking phenomenon occurs if 8-noded element is used for small thickness/span ratios with coarse mesh, but shear-locking phenomenon does not occur if finer mesh is used. As also seen from these tables and figures, shear-locking phenomenon does not occur if 17-noded element is used for any values of thickness/span ratios. No matter the mesh is coarse or fine. Also, the exact result can approximately be obtained with the full integration.

In general, the results obtained in this study are better than the results given in the literature.

In order to help the researchers, the maximum values of displacements and bending moments of MT17 element for 8×8 mesh sizes (64 elements) for different aspect ratios are also presented in this study. The maximum displacements, bending moments M_x and M_y at the center of the plates, and bending moment M_x and M_y at the center of the edge in the x and y directions, respectively, for different aspect ratios are given in Table 5 for clamped plates and in Table 6 for simply supported plates. These values are also presented in graphical form in Figs. 7, 8, 9, 10, and 11, respectively.

Table 5 Absolute maximum displacements and bending moments of clamped plates for different aspect ratios

b/a	w at center (mm)	M_x at center (kNmm)	M_x at center of edge in y direction (kNmm)	M_y at center (kNmm)	M_y at center of edge in x direction (kNmm)
1.0	0.0365	-4175	8667	-4175	8667
1.5	0.0613	-6631	13153	-3748	9656
2.0	0.0702	-7421	14585	-2910	9646
3.0	0.0723	-7549	14807	-2290	9625

Table 6 Absolute maximum displacement and bending moments of simply supported plates for different aspect ratios

b/a	w at center (mm)	M_x at center (kNmm)	M_y at center (kNmm)
1.0	0.1120	-9171	-9171
1.5	0.2056	-15303	-9333
2.0	0.2632	-18883	-8520
3.0	0.3100	-21674	-7331

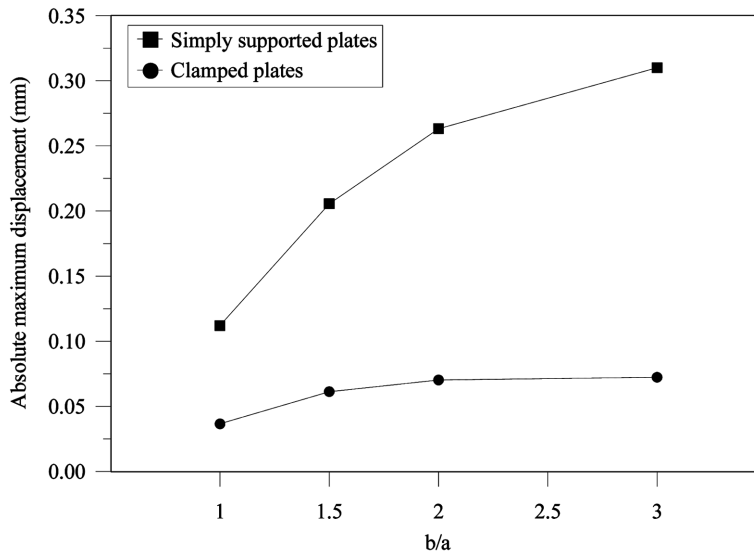
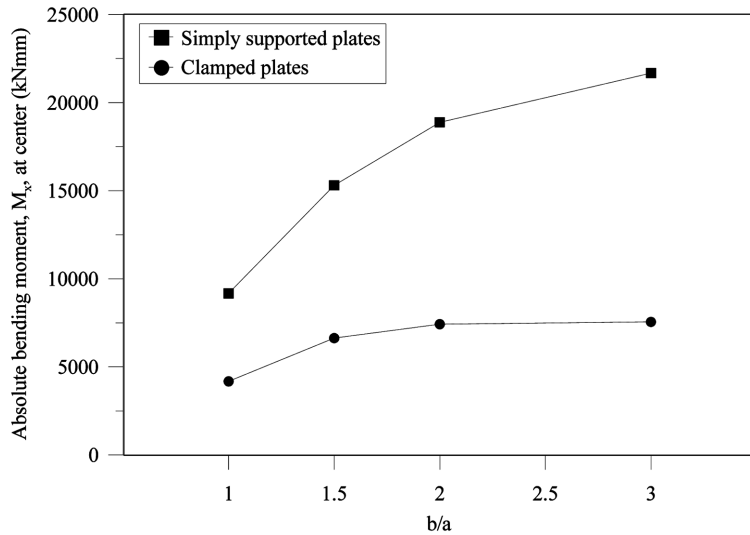
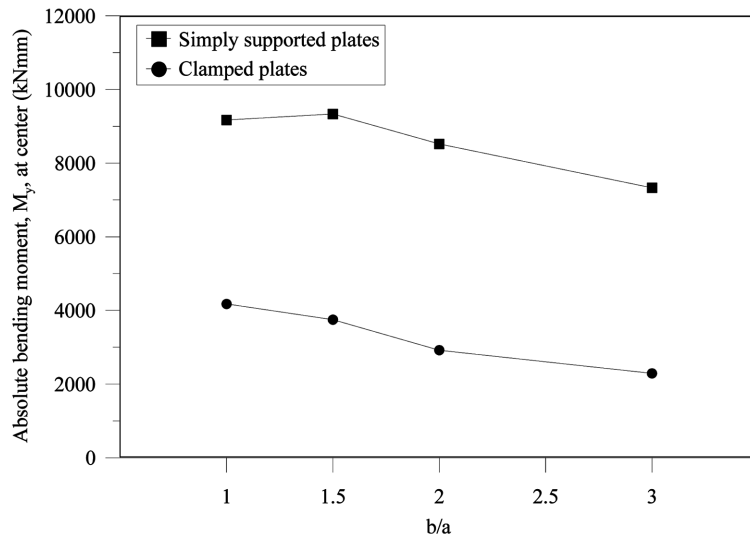


Fig. 7 Absolute maximum displacement of the plates for different aspect ratios

As seen from Table 5, and 6 and Fig. 7, the maximum displacements of simply supported plates are larger than those of clamped plates. The maximum displacements increase while aspect ratios increase. This increase is larger for the small values of the aspect ratios. In other words, the increases in the maximum displacements decrease with increasing aspect ratio.

As seen from Table 5, and 6 and Fig. 8, the maximum bending moments, M_x , at the center of

Fig. 8 Absolute bending moment, M_x , at center of the plates for different aspect ratiosFig. 9 Absolute bending moment, M_y , at center of the plates for different aspect ratios

simply supported plates are larger than those of clamped plates. The maximum bending moments M_x at the center increase while aspect ratios increase. This increase is larger for the small values of the aspect ratios. In other words, the increases in the maximum bending moments decrease with increasing aspect ratio.

As seen from Table 5, and 6 and Fig. 9, the maximum bending moments, M_y , at the center of simply supported plates are larger than those of clamped plates. In general, the maximum bending moments M_y at the center decrease while aspect ratios increase. Degree of decreases change depending on the aspect ratio.

As seen from Table 5 and Fig. 10, the maximum bending moment M_x at the center of the edge in

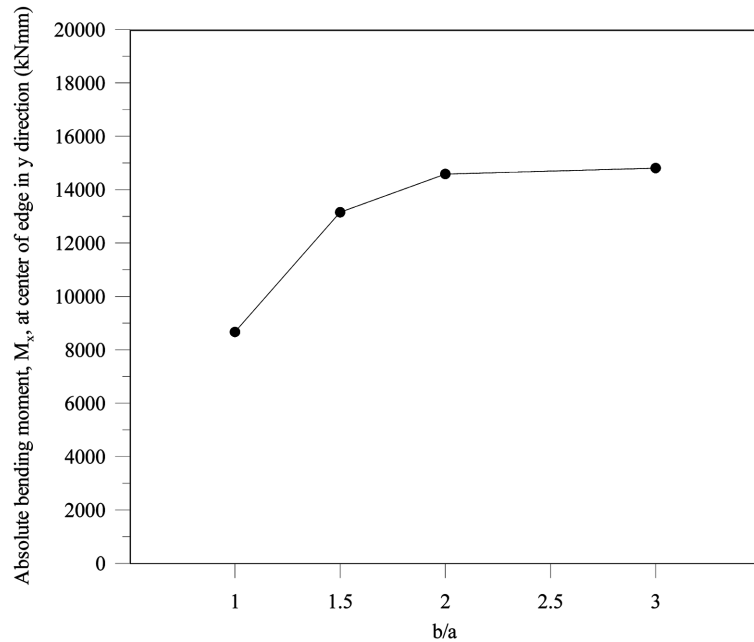


Fig. 10 Absolute bending moment, M_x , at the center of the edge in the y direction of the clamped plates for different aspect ratios

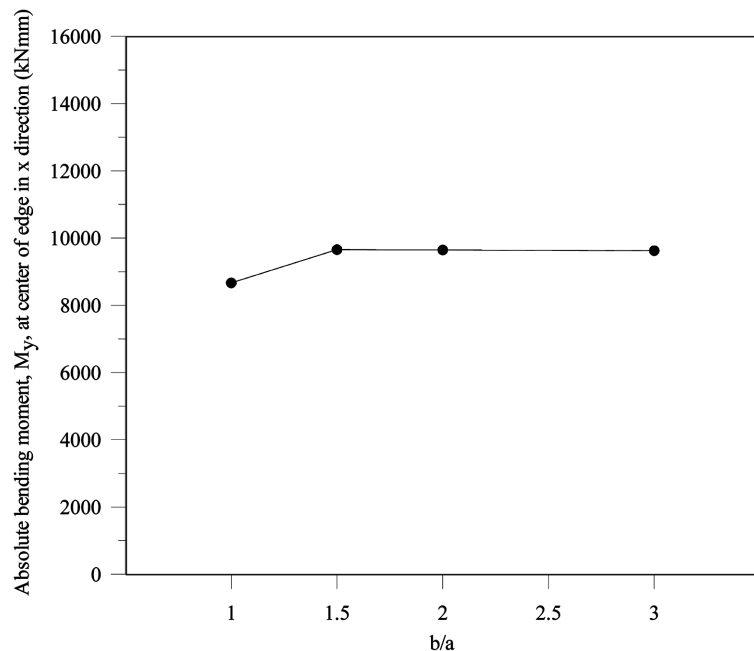


Fig. 11 Absolute bending moment, M_y , at the center of the edge in the x direction of the clamped plates for different aspect ratios

the y direction of the clamped plates increase while aspect ratios increase. This increase is larger for the small values of the aspect ratios. If the aspect ratios become large, the increase in this M_x can be ignored.

As seen from Table 5 and Fig. 11, the maximum bending moment M_y at the center of the edge in the x direction of the clamped plates increase while aspect ratio increases, but this increase is negligible after the aspect ratio of 1.5.

5. Conclusions

In this paper, shear-locking free analysis of thick plates is studied by using 8-and 17-noded finite elements and the maximum displacements and bending moments of the plates along all four edges clamped and simply supported are obtained. The results are compared with the results given in the literature. It is concluded that, by using 17-noded finite element, the mesh size required to produce the desired accuracy can be approximately reduced to the half of those of the others given in the literature. The results obtained by using 17-noded finite element almost coincide with the exact result for any mesh sizes. Also, shear-locking phenomenon does not occur if 17-noded element is used for any values of thickness/span ratios. No matter the mesh is course or fine. The exact result can approximately be obtained with the full integration. The results of this study are better than the results given in the literature if they are compared with the exact results. In addition, the following conclusions which are known by the researchers in this field can also be drawn from the results obtained in this study.

The maximum displacements of the thick plates increase as the aspect ratio increases.

The bending moments M_x at the center of the plates increase with increasing aspect ratios.

The bending moments M_y at the center of the plates decrease with increasing aspect ratios.

The bending moments M_x at the center of the edge in the y direction of the plates increase with increasing aspect ratios.

The bending moments M_y at the center of the edge in the x direction almost remain the same as the aspect ratios increase.

Degree of decreases or increases decreases with increasing aspect ratios.

Acknowledgements

This study is a part of Ph. D. Thesis of Yaprak Itr Özdemir, and it is supported by the Research Fund of Karadeniz Technical University. Project number: 2002.112.1.5.

References

- Ayvaz, Y. (1992), *Parametric Analysis of Reinforced Concrete Slabs Subjected to Earthquake Excitation*, Ph. D. Thesis, Graduate School of Texas Tech University, Lubbock, Texas.
- Bathe, K.J. (1996), *Finite Element Procedures*, Prentice Hall, Upper Saddle River, New Jersey.
- Batoz, J.L. and Tahar, M.B. (1982), "Evaluation of a new quadrilateral thin plate bending elements", *Int. J. Num. Meth. Eng.*, **18**, 1655-1677.

- Belounar, L. and Guenfoud, M. (2005), "A new rectangular finite element based on the strain approach for plate bending", *Thin Wall. Struct.*, **43**(1), 47-63.
- Cai, L., Rong, T. and Chen, D. (2002), "Generalized mixed variational methods for reissner plate and its application", *Comput. Mech.*, **30**, 29-37.
- Cen, S., Long, Y., Yao, Z. and Chiew, S. (2006), "Application of the quadrilateral area coordinate method", *Int. J. Num. Eng.*, **66**, 1-45.
- Cook, R.D., Malkus, D.S. and Michael, E.P. (1989), *Concepts and Applications of Finite Element Analysis*. John Wiley & Sons, Inc., Canada.
- Çelik, M. (1996), *Plak sonlu elemanlarda kayma şekildeğiştirmelerinin gözönüne alınması ve iki parametreli zemine oturan plakların hesab için bir yöntem*, Ph. D. Thesis, Istanbul Technical University, Istanbul.
- Ibrahimbegovic, A. (1993), "Quadrilateral finite elements for analysis of thick and thin plates", *Comput. Meth. Appl. M.*, **110**, 195-209.
- Lovadina, C. (1996), "A new class of mixed finite element methods for Reissner-Mindlin Plates", *SIAM J. Numer. Anal.*, **33**, 2457-2467.
- Mindlin, R.D. (1951), "Influence of rotatory inertia and shear on flexural motions of isotropic, elastic plates", *J. Appl. M.*, **18**, 31-38.
- Owen, D.R.J. and Zienkiewicz, O.C. (1982), "A refined higher-order C^0 plate bending element", *Comput. Struct.*, **15**, 83-177.
- Ozkul, T.A. and Ture, U. (2004), "The transition from thin plates to moderately thick plates by using finite element analysis and the shear locking problem", *Thin Wall. Struct.*, **42**, 1405-1430.
- Özdemir, Y.I. and Ayvaz, Y. (2004), "Analysis of clamped and simply supported thick plates using finite element method", *Proc. of the 6th Int. Cong. on Advances in Civil Engineering*, Istanbul, **1**, 652-661.
- Panc, V. (1975), *Theory of Elastic Plates*, Noordhoff, Leiden.
- Reissner, E. (1947), "On bending of elastic plates", *Q. Appl. Math.*, **5**, 55-68.
- Reissner, E. (1950), "On a variational theorem in elasticity", *J. Math. Phys.*, **29**, 90-95.
- Soh, A.K., Cen, S., Long, Y. and Long, Z. (2001), "A new twelve DOF quadrilateral element for analysis of thick and thin plates", *Eur. J. Mech.; A-Solids*, **20**, 299-326.
- Timoshenko, S. and Woinowsky-Krieger, S. (1959), *Theory of Plates and Shells. Second edition*, McGraw-Hill., New York.
- Ugural, A.C. (1981), *Stresses in Plates and Shells*, McGraw-Hill, New York.
- Wanji, C. and Cheung, Y.K. (2000), "Refined quadrilateral element based on Mindlin/Reissner plate theory", *Int. J. Numer. Meth. Eng.*, **47**, 605-627.
- Weaver, W. and Johnston, P.R. (1984), *Finite Elements for Structural Analysis*, Prentice Hall, Inc., Englewood Cliffs, New Jersey, 200-212.
- Weaver, W. and Johnston, P.R. (1984), *Finite Elements for Structural Analysis*, Prentice Hall, Englewood Cliffs; New Jersey.
- Yuan, F.-G. and Miller, R.E. (1988), "A rectangular finite element for moderately thick flat plates", *Comput. Struct.*, **30**, 1375-1387.
- Yuan, F.-G. and Miller, R.E. (1989), "A cubic triangular finite element for flat plates with shear", *Int. J. Num. Eng.*, **18**(1), 1-15.
- Yuqiu, L. and Fei, X. (1992), "A universal method for including shear deformation in thin plates elements", *Int. J. Num. Eng.*, **34**, 171-177.
- Zienkiewicz, O.C., Xu, Z., Ling, F.Z. and Samuelsson, A. (1993), "Linked interpolation for Reissner-Mindlin plate element: Part I-a simple quadrilateral", *Int. J. Num. Meth. Eng.*, **36**, 3043-3056.

Appendix

For 8-noded element

$$[B]_{24 \times 5}^T = \begin{bmatrix} 0 & 0 & 0 & \frac{\partial h_1}{\partial x} & \frac{\partial h_1}{\partial y} \\ 0 & \frac{\partial h_1}{\partial y} & \frac{\partial h_1}{\partial x} & 0 & h_1 \\ -\frac{\partial h_1}{\partial x} & 0 & -\frac{\partial h_1}{\partial y} & -h_1 & 0 \\ 0 & 0 & 0 & \frac{\partial h_2}{\partial x} & \frac{\partial h_2}{\partial y} \\ 0 & \frac{\partial h_2}{\partial x} & \frac{\partial h_2}{\partial x} & 0 & h_2 \\ -\frac{\partial h_2}{\partial x} & 0 & -\frac{\partial h_2}{\partial y} & -h_2 & 0 \\ 0 & 0 & 0 & \frac{\partial h_3}{\partial x} & \frac{\partial h_3}{\partial y} \\ 0 & \frac{\partial h_3}{\partial x} & \frac{\partial h_3}{\partial x} & 0 & h_3 \\ -\frac{\partial h_3}{\partial x} & 0 & -\frac{\partial h_3}{\partial y} & -h_3 & 0 \\ 0 & 0 & 0 & \frac{\partial h_4}{\partial x} & \frac{\partial h_4}{\partial y} \\ 0 & \frac{\partial h_4}{\partial x} & \frac{\partial h_4}{\partial x} & 0 & h_4 \\ -\frac{\partial h_4}{\partial x} & 0 & -\frac{\partial h_4}{\partial y} & -h_4 & 0 \\ 0 & 0 & 0 & \frac{\partial h_5}{\partial x} & \frac{\partial h_5}{\partial y} \\ 0 & \frac{\partial h_5}{\partial x} & \frac{\partial h_5}{\partial x} & 0 & h_5 \\ -\frac{\partial h_5}{\partial x} & 0 & -\frac{\partial h_5}{\partial y} & -h_5 & 0 \\ 0 & 0 & 0 & \frac{\partial h_6}{\partial x} & \frac{\partial h_6}{\partial y} \\ 0 & \frac{\partial h_6}{\partial x} & \frac{\partial h_6}{\partial x} & 0 & h_6 \\ -\frac{\partial h_6}{\partial x} & 0 & -\frac{\partial h_6}{\partial y} & -h_6 & 0 \\ 0 & 0 & 0 & \frac{\partial h_7}{\partial x} & \frac{\partial h_7}{\partial y} \\ 0 & \frac{\partial h_7}{\partial x} & 0 & 0 & h_7 \\ -\frac{\partial h_7}{\partial x} & 0 & -\frac{\partial h_7}{\partial y} & -h_7 & 0 \\ 0 & 0 & 0 & \frac{\partial h_8}{\partial x} & \frac{\partial h_8}{\partial y} \\ 0 & \frac{\partial h_8}{\partial x} & 0 & 0 & h_8 \\ -\frac{\partial h_8}{\partial x} & 0 & -\frac{\partial h_8}{\partial y} & -h_8 & 0 \end{bmatrix}$$

For 17-noded element

0	0	0	$\frac{\partial h_1}{\partial x}$	$\frac{\partial h_1}{\partial y}$
0	$\frac{\partial h_1}{\partial y}$	$\frac{\partial h_1}{\partial x}$	0	h_1
$-\frac{\partial h_1}{\partial x}$	0	$-\frac{\partial h_1}{\partial y}$	$-h_1$	0
0	0	0	$\frac{\partial h_2}{\partial x}$	$\frac{\partial h_2}{\partial y}$
0	$\frac{\partial h_2}{\partial x}$	$\frac{\partial h_2}{\partial x}$	0	h_2
$-\frac{\partial h_2}{\partial x}$	0	$-\frac{\partial h_2}{\partial y}$	$-h_2$	0
0	0	0	$\frac{\partial h_3}{\partial x}$	$\frac{\partial h_3}{\partial y}$
0	$\frac{\partial h_3}{\partial x}$	$\frac{\partial h_3}{\partial x}$	0	h_3
$-\frac{\partial h_3}{\partial x}$	0	$-\frac{\partial h_3}{\partial y}$	$-h_3$	0
0	0	0	$\frac{\partial h_4}{\partial x}$	$\frac{\partial h_4}{\partial y}$
0	$\frac{\partial h_4}{\partial x}$	$\frac{\partial h_4}{\partial x}$	0	h_4
$-\frac{\partial h_4}{\partial x}$	0	$-\frac{\partial h_4}{\partial y}$	$-h_4$	0
0	0	0	$\frac{\partial h_5}{\partial x}$	$\frac{\partial h_5}{\partial y}$
0	$\frac{\partial h_5}{\partial x}$	$\frac{\partial h_5}{\partial x}$	0	h_5
$-\frac{\partial h_5}{\partial x}$	0	$-\frac{\partial h_5}{\partial y}$	$-h_5$	0
0	0	0	$\frac{\partial h_6}{\partial x}$	$\frac{\partial h_6}{\partial y}$
0	$\frac{\partial h_6}{\partial x}$	$\frac{\partial h_6}{\partial x}$	0	h_6
$-\frac{\partial h_6}{\partial x}$	0	$-\frac{\partial h_6}{\partial y}$	$-h_6$	0
0	0	0	$\frac{\partial h_7}{\partial x}$	$\frac{\partial h_7}{\partial y}$
0	$\frac{\partial h_7}{\partial x}$	0	0	h_7
$-\frac{\partial h_7}{\partial x}$	0	$-\frac{\partial h_7}{\partial y}$	$-h_7$	0
0	0	0	$\frac{\partial h_8}{\partial x}$	$\frac{\partial h_8}{\partial y}$
0	$\frac{\partial h_8}{\partial x}$	0	0	h_8
$-\frac{\partial h_8}{\partial x}$	0	$-\frac{\partial h_8}{\partial y}$	$-h_8$	0
0	0	0	$\frac{\partial h_9}{\partial x}$	$\frac{\partial h_9}{\partial y}$
0	$\frac{\partial h_9}{\partial x}$	0	0	h_9
$-\frac{\partial h_9}{\partial x}$	0	$-\frac{\partial h_9}{\partial y}$	$-h_9$	0

Continued

0	0	0	$\frac{\partial h_{10}}{\partial x}$	$\frac{\partial h_{10}}{\partial y}$
0	$\frac{\partial h_{10}}{\partial y}$	$\frac{\partial h_{10}}{\partial x}$	0	h_{10}
$\frac{\partial h_{10}}{\partial x}$	0	$-\frac{\partial h_{10}}{\partial y}$	$-h_{10}$	0
0	0	0	$\frac{\partial h_{11}}{\partial x}$	$\frac{\partial h_{11}}{\partial y}$
0	$\frac{\partial h_{11}}{\partial x}$	$\frac{\partial h_{11}}{\partial x}$	0	h_{11}
$\frac{\partial h_{11}}{\partial x}$	0	$-\frac{\partial h_{11}}{\partial y}$	$-h_{11}$	0
0	0	0	$\frac{\partial h_{12}}{\partial x}$	$\frac{\partial h_{12}}{\partial y}$
0	$\frac{\partial h_{12}}{\partial x}$	$\frac{\partial h_{12}}{\partial x}$	0	h_{12}
$\frac{\partial h_{12}}{\partial x}$	0	$-\frac{\partial h_{12}}{\partial y}$	$-h_{12}$	0
0	0	0	$\frac{\partial h_{13}}{\partial x}$	$\frac{\partial h_{13}}{\partial y}$
0	$\frac{\partial h_{13}}{\partial x}$	$\frac{\partial h_{13}}{\partial x}$	0	h_{13}
$\frac{\partial h_{13}}{\partial x}$	0	$-\frac{\partial h_{13}}{\partial y}$	$-h_{13}$	0
0	0	0	$\frac{\partial h_{14}}{\partial x}$	$\frac{\partial h_{14}}{\partial y}$
0	$\frac{\partial h_{14}}{\partial x}$	$\frac{\partial h_{14}}{\partial x}$	0	h_{14}
$\frac{\partial h_{14}}{\partial x}$	0	$-\frac{\partial h_{14}}{\partial y}$	$-h_5$	0
0	0	0	$\frac{\partial h_{15}}{\partial x}$	$\frac{\partial h_{15}}{\partial y}$
0	$\frac{\partial h_{15}}{\partial x}$	$\frac{\partial h_{15}}{\partial x}$	0	h_{15}
$\frac{\partial h_{15}}{\partial x}$	0	$-\frac{\partial h_{15}}{\partial y}$	$-h_{15}$	0
0	0	0	$\frac{\partial h_{16}}{\partial x}$	$\frac{\partial h_{16}}{\partial y}$
0	$\frac{\partial h_{16}}{\partial x}$	0	0	h_{16}
$\frac{\partial h_{16}}{\partial x}$	0	$-\frac{\partial h_{16}}{\partial y}$	$-h_{16}$	0
0	0	0	$\frac{\partial h_{17}}{\partial x}$	$\frac{\partial h_{17}}{\partial y}$
0	$\frac{\partial h_{17}}{\partial x}$	0	0	h_{17}
$\frac{\partial h_{17}}{\partial x}$	0	$-\frac{\partial h_{17}}{\partial y}$	$-h_{17}$	0